JP0350244

1.3.1 POSITRON ANNIHILATION STUDIES ON BULK METALLIC GLASS AND HIGH INTENSITY POSITRON BEAM DEVELOPMENTS

P. Asoka-Kumar* and W. Stoeffl
Lawrence Livermore National Laboratory, Livermore, CA 94550 USA

Abstract

Positron annihilation spectroscopy is an ideal probe to examine atomic scale open-volume regions in materials. Below, we summarize the recent results on studies of open-volume regions of a multicomponent Zr-Ti-Ni-Cu-Be bulk metallic glass. Our studies establish two types of open-volume regions, one group that is too shallow to trap positrons at room temperature and becomes effective only at low temperatures and the other group that localizes positrons at room temperature and is large enough to accommodate hydrogen. The second half of the paper will concentrate on the high intensity positron program at Lawrence Livermore National Laboratory. A new positron production target is under development and we are constructing two experimental end stations to accommodate a pulsed positron microprobe and an experiment on positron diffraction and holography. Important design considerations of these experiments will be described.

Keywords: metallic glass, positron production, positron microprobe, positron diffraction and holography

1. Introduction

The use of positron beams in surface and materials science offers unique opportunities to obtain detailed information on defects and electronic properties of materials[1-5]. Since the initial discovery of "moderation", the process by which a small portion of positrons incident on a material with a negative positron work function is reemitted with narrow energy and angular distributions, several monoenergetic positron beam systems has been developed. At Lawrence Livermore National Laboratory, we are operating and developing several positron beam systems that are capable of examining materials at different depth scales and sampling volumes. Below, we summarize the results obtained with high-energy positron beams and new developments to build a multi-user experimental program using a high-intensity, low-energy positron beam.

A high-energy positron beam is formed using positrons emitted from a ^{22}Na source placed at the terminal of a 3 MeV electrostatic accelerator[6]. The positron beam (with a typical intensity of $5x10^5$ positrons/sec) emerging from the accelerator column is focused by a thin solenoid, exits the vacuum through a 25 μm thick Al window, and enters the specimen either directly or after passing through a 2 mm thick scintillator, that provides a start signal for positron lifetime measurements. The positron penetration depth into the test material is greater than 2-3 mm and allows us to measure bulk properties without significant contributions from the near-surface regions. The annihilation spectrum is detected with detectors positioned collinear or perpendicular to the incoming positron beam direction. A collinear geometry is often used in lifetime measurements, while a perpendicular geometry allows both lifetime and energy analysis

* Corresponding Author, E-mail Address: asoka@llnl.gov

using coincidence logic between the annihilation gamma rays. Since the beam exits the vacuum system, the setup is convenient to probe engineering materials with specialized fixtures, encapsulated samples requiring a specific environment, and liquids. Recently, we have applied this system to study diverse problems such as embrittlement in reactor pressure vessel steels[7], direct observation of carbon-decorated defects in fatigued type 304 stainless steel[8], preferential positron sampling of anions in alkali halides[9], and characterization of open-volume regions in bulk metallic glass[10-13]. In section 2, we summarize results obtained from bulk metallic glass.

The high intensity positron program is summarized in section 3. The primary source of positrons is built at the end of a 100 MeV linear accelerator, capable of delivering up to 40 kilo Watt peak power at a repetition rate of up to 1400 Hz. At present, the positron program is well integrated into the core mission of the 100 MeV accelerator and is expected to be available for positron studies and associated collaborative experiments for about 4-6 months a year.

2. Free volume characterization in bulk metallic glass

A new class of multi-component metallic glasses that can be grown in bulk form at relatively slow cooling rates have attracted considerable commercial and technological interest[14,15]. These glasses exhibit a number of attractive physical and mechanical properties, including large elastic strains to failure, high tensile strengths, and excellent wear and corrosion resistances. Open volume regions in glassy structures are known to play an important role in determining and modifying their properties when subjected to various external conditions. Positron annihilation spectroscopy is a highly sensitive, nondestructive probe to study the nature, concentration, and spatial distribution of open volume regions in materials. Positron lifetimes are influenced by the presence of these open volume regions and can be used to measure the "openness" of these frozen-in disordered regions. A number of studies in conventional rapidly quenched metallic glasses yield single-component lifetime spectrum with a decay constant indicative of open volume regions that are smaller than the vacancies found in constituent metals[16].

Electron momentum distributions in a solid can be examined using the Doppler shift of annihilation gamma rays[1]. The high momentum part of this spectrum (denoted as OEMS, Orbital Electron Momentum Spectrum) is dominated by orbital electrons that retain their atomic character and are thus elemental specific[17-19]. The elemental specificity of OEMS has been employed successfully to address many defect-related problems[20-23].

We have used positron lifetime and OEMS measurements to characterize open volume regions in two sets of Zr-based five-component alloys, $Zr_{52.5}Ti_5Al_{10}Cu_{17.9}Ni_{14.6}$ and $Zr_{41.25}Ti_{13.75}Ni_{10}Cu_{12.5}Be_{22.5}$. They yield similar lifetime values of 177±3 ps and 179.5±0.5 ps, respectively. Similar to conventional metallic glass, these lifetime values lie between those observed for bulk constituent metals and metal vacancies, suggesting positrons are sampling quenched-in open volume regions that are smaller than metal vacancies.

OEMS measurements conducted as a function of sample temperature confirm that positrons are localized at open volume regions and are not distributed throughout the alloy. Fig. 1

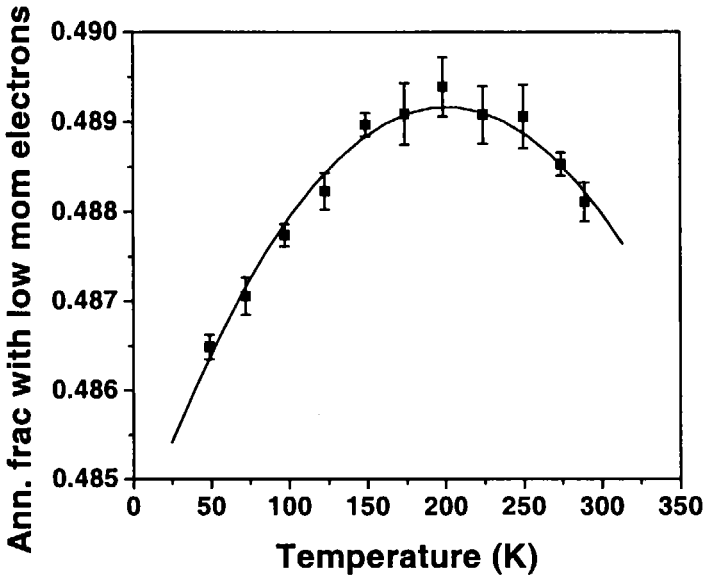

Figure 1. The plot shows the fraction of positrons annihilating with low momentum electrons (< 0.38 atomic units, with a system resolution of 0.38 atomic units) as a function of the sample temperature. The solid line through the data points is a guide to the eye.

shows the fraction of positrons annihilating with low momentum (< 0.38 atomic units, a.u.) electrons as a function of temperature. As the temperature is reduced from ambient, the fraction of positrons annihilating with low momentum electrons increases first, reaches a peak value at ~ 200 K, before decreasing and showing an opposite trend at temperatures below 200K. The positrons sample low momentum electrons more effectively when they are localized at open volume regions. These measurements suggest that there are at least two groupings of open volume sizes in these materials. The first group is more open and is barely deep enough to produce positron binding at room temperature, while the second group is shallow and binds positrons only at low temperatures. At room temperature, positron binding to open volume regions with large mean size is not complete and as the temperature approaches ~ 200 K, positron thermal energy is not sufficient to cause significant detrapping. At temperatures below 200 K, the second group with higher number density dominates the observed positron features. Similar positron measurements from samples charged with hydrogen show that open-volume regions that are localizing positrons at room temperature can also accommodate hydrogen[10].

A two-hour annealing at 650 °C (above the crystallization temperature, 470 °C) of the Al containing alloy reduced the lifetime to a value of 172±2 ps. The small changes upon annealing suggest that the crystallized sample contains many phases with a high concentration of positron localization sites, such as dislocations and grain boundaries and positrons are easily transported through the grains. A long anneal (48 hours at 500 °C) of the Be containing alloy reduced the lifetime value to 164.5±0.5 ps. However, calculated lifetime values for some of the known phases $NiZr_2$ and Zr_2Cu were 143 and 151 ps, respectively[24], significantly shorter than the experimental lifetime value, suggesting positron localization at open volume regions and not at crystallized regions.

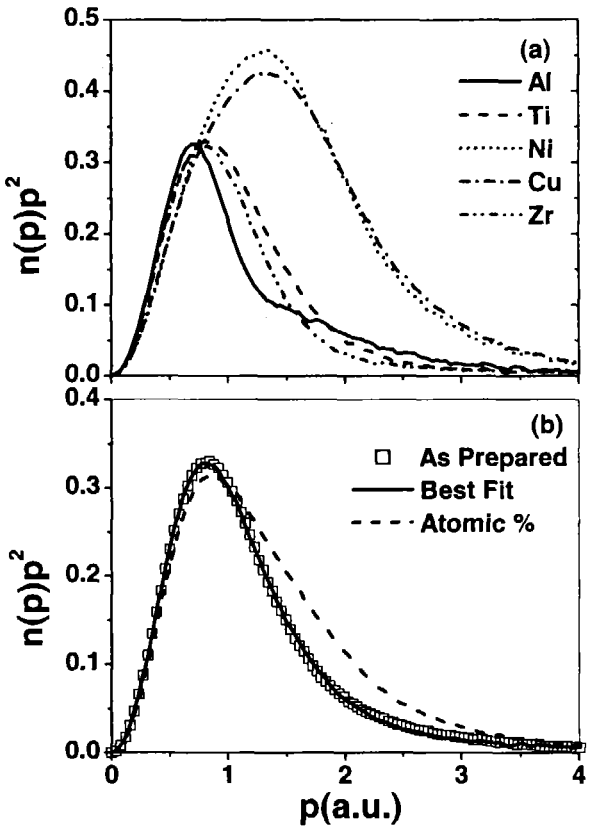

Figure 2. The top panel (a) shows the electron momentum distribution of constituent elements weighted with p^2 to enhance the features associated with orbital electrons at high momentum values. The bottom panel (b) shows the momentum distribution of $Zr_{41.25}Ti_{13.75}Ni_{10}Cu_{12.5}Be_{22.5}$. Broken line represents a perfect random distribution of elements around the positron annihilation site. The solid curve corresponds to the best fit obtained by adjusting the contributions from different elements shown in panel (a).

Detailed comparison of the OEMS spectra corresponding to the amorphous metal and metallic sub components show significant chemical ordering around open-volume regions[24]. Our results show that Ni and Cu atoms closely occupy the volume bounded by their neighboring atoms, while Be, Al, Ti, and Zr are less closely packed, and more likely to be associated with the open volume regions. Fig. 2 shows the OEMS spectra for constituent metals and best fit obtained by using a linear combination of the individual contributions. Also shown is a curve that corresponds to a linear combination in which the positron wave function is sampling a perfect random distribution of the constituents. The fitted coefficients are shown in Fig. 3. Ti contribution is enhanced to ~30% from a value of 5%. Contributions from Ni and Cu are combined and are reduced from 32.5% to 8%. Zr and Al contribution are comparable to grown-in concentration. These results show that open volume regions sampled by positrons are surrounded by atoms like Ti, Zr, and Al. Similar results are obtained in Be containing alloy where Be replaces the role of Al[12].

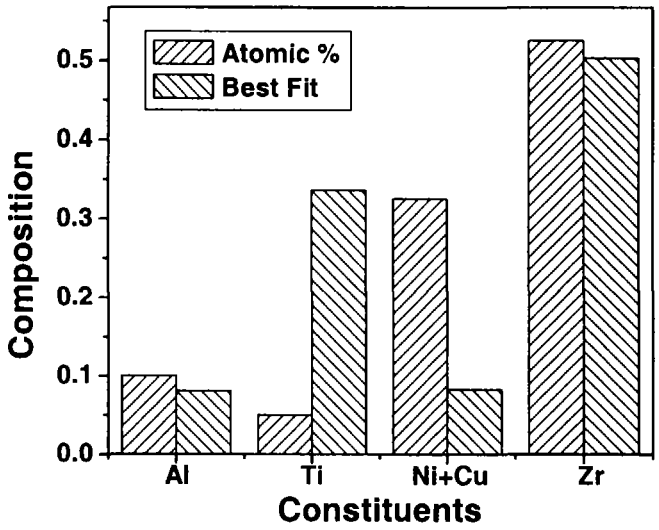

Figure 3. Composition of constituent elements as revealed by positron annihilation measurements. Compared to the grown-in concentration, Ti is enhanced at the expense of Ni and Cu.

3. High Intensity Positron Program at LLNL

A large number of experiments can benefit from a high-intensity, low-energy positron beam. At present the low energy positron beam capabilities at US National Laboratories are led by the efforts at Lawrence Livermore National Laboratory. We are building a state-of-the-art multi user experimental program to meet the needs of the scientific community. Below we summarize the design features of the positron production area and some of the experiments planned for the immediate future.

The layout of the experimental hall, positron production hall, and linear electron accelerator (linac) is shown in Fig. 4. Positrons are produced at the end of a 100 MeV linac. The linac vacuum system is not connected to the positron vacuum system and electrons exit the linac system through a thin, water-cooled window and enter the positron vacuum system. The entrance vacuum window is integrated with a well-cooled stopping target for electrons. In the previous design[25], the stopping target was outside the vacuum system and physically decoupled from the vacuum window. Thus, the vacuum window to the positron production chamber was located downstream of the Bremstrahlung shower and suffered significant degradation at high power and was not able to withstand the sustained linac operation. In addition, the close proximity of the stopping target and vacuum window caused electrical arcing during the short linac pulse cycle, causing further degradation. In our current design, the vacuum window will face the electron beam first and thus will overcome the electrical arcing problem.

Immediately following the stopping target is an option to add either a flat tungsten foil or a set of tungsten foils of different geometry (like vanes) to increase the overall positron emission area. Initial tests conducted at low power will optimize the geometry for both phase space and

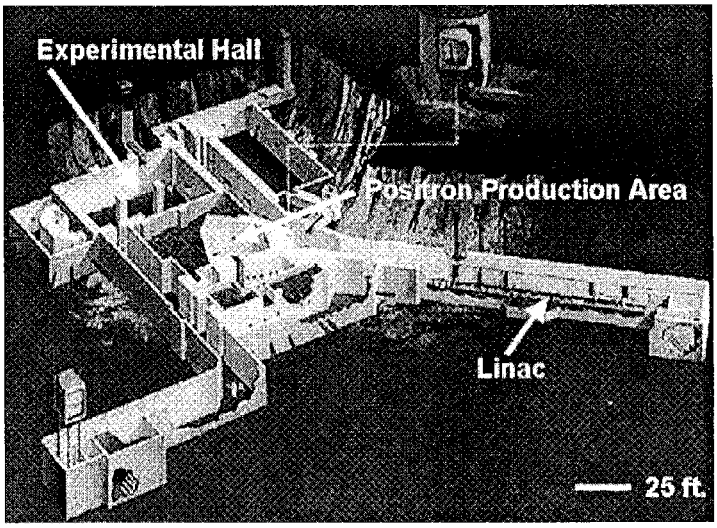

Figure 4. The layout of the intense positron beam at Lawrence Livermore National Laboratory. Positrons are produced at the end of a 100 MeV linac and transported to the experimental hall using a guiding magnetic field.

intensity. New design also allows easy interchange of the entrance window with fixtures incorporating in situ heating of the tungsten foil using direct electrical current flowing through them. We intend to study the effects of foil temperature on positron emission characteristics at low linac power to understand the relationship between the dynamic annealing of beam-induced defects and positron emission characteristics[26]. The tungsten foil temperature during a high power linac pulse is expected to be well above migration energies of simple defects in tungsten. We also have installed additional ports for introducing trace amounts of gases to study their effects on positron conversion efficiency. Another design criteria is to keep all surfaces exposed and close to the primary tungsten foil to be made out of tungsten to prevent sputter deposition of foreign elements. In our previous design, we observed significant coatings formed from sputtered aluminum and tungsten during high power linac operation.

A fraction of positrons that are slowed down near the surface of the tungsten foils will get reemitted as moderated positrons. These positrons are harvested and transported to an experimental hall with a guiding magnetic field. The beam transport system contains a curved section to prevent direct line of sight from the source region. The experimental hall and the positron production area are separated by 4.5 m of concrete shielding to ensure a low radiation background in the experimental hall. At the end of the curved section (in the positron production hall), we have also installed a ^{22}Na source (~15 mCi) and a tungsten moderator foil. This new source-moderator assembly provides a low intensity positron beam for test and setup purpose and can be withdrawn during high intensity beam operation. Both the high intensity and low intensity positron beam can be transported to the experimental hall at energies of ~ 10 eV to 10 keV.

The positron beam entering the experimental hall can be transported to multiple end stations, including positron microprobe, positron diffraction and holography, and a OEMS chamber. Some of the experiments (OEMS) will use the low intensity beam exclusively, while

the others will use the high intensity beam with further conditioning to alter their time structure and phase space properties.

The positron microprobe will produce a tunable (~ 1keV to 50 keV), time-bunched (100 ps wide, 20 MHz) positron beam with a pot size of ~ 1 μm and can be used to obtain a three dimensional maps of defects in materials. Some of the novel features associated with our microprobe design can be found elsewhere[27]. The time structure of the initial positron beam is decided by the primary electron beam and is not suited for positron microprobe since it will saturate most detector systems. Therefore positrons produced by each linac pulse are captured, time stretched, and rebunched to provide suitable time structure for the micropobe[28]. To compress the beam spot from an initial diameter of 1 cm to ~ 1 μm, we will also employ several stages of remoderation. Overall efficiency of the transport system and 3-stage remoderation stages is expected to be of the order of 10^{-3}, and hence we expect a beam intensity of more than 10^6 positrons/sec at the target.

The intense positron beam is ideal for positron diffraction and holography measurement. The advantages of a positron beam over an electron beam in terms of fewer artifacts and ambiguities in the diffraction pattern are well known[2]. However, lack of a sufficiently intense positron beam has hindered previous attempts to take full advantage of the positron diffraction for surface characterization. A serious disadvantage posed by a positron diffraction experiment over an electron diffraction experiment is the background caused by the prolific emission of positronium (a neutral bound state of an electron and a positron) from the sample surface. Since positronium is neutral it will pass through the grid system located in front of the channel plate detector system. In standard electron diffraction experiment, the grid system is used to suppress the electrons scattered inelastically and is used to perform similar functions in a positron diffraction experiment. To overcome issued associated with positronium background, we will take advantage of the pulsed nature of the positron beam. Since positronium signal will reach the channel plate at a later time compared to the elastically scattered positrons contributions arising form inelastic scattering and positronium can be discarded.

We summarized the intense positron beam development at Lawrence Livermore National Laboratory. The high flux of the LLNL beam and the assortment of spectroscopic tools being developed will enable several unique experiments.

We would like to thank R.H. Dauskardt, K.M. Flores, R. Howell, T.G. Nieh, D. Schneider, P.A. Sterne, and D. Suh for many useful discussions. This work was performed under the auspices of the U.S. Department of Energy by the University of California at Lawrence Livermore National Laboratory under contract No. W-7405-Eng-48. Part of this work was also supported by Basic Energy Research, Materials Science Division of U.S. Department of Energy.

References

1. R .Krauuse-Rehber and H.S. Leipner, *Positron Annihilation in Semi-conductors* (Springer, Berlin, 1999).
2. S.Y. Tong, H. Huang, and X.Q. Guo, Phys. Rev. Lett., **69**, 3654 (1992).
3. P. Asoka-Kumar, K.G. Lynn, and D.O. Welch, J. Appl. Phys., **76**, 4935 (1994).

4. A. David, G. Kögel, P. Sperr, and W. Triftshäuser, Phys. Rev. Lett., **87**, 067402 (2001).
5. M.J. Puska and R.M. Nieminen, Rev. Mod. Phys., **66**, 841 (1994).
6. R.H. Howell, P.A. Sterne, J. Hartley, T.E. Cowan, Appl. Surf. Sci., **149**, 103 (1999).
7. P. Asoka-Kumar, R. Howell, T.G. Nieh, P.A. Sterne, B.D. Wirth, R.H. Dauskardt, K.M. Flores, D. Suh, and G.R. Odette, Appl. Surf. Sci., in print (2002).
8. P. Asoka-Kumar, J.H. Hartley, R.H. Howell, P.A. Sterne, D. Akers, V. Shah, and A. Denison, Acta Materialia, in press (2002).
9. J.H. Hartley, P. Asoka-Kumar, R.H. Howell, P.A. Sterne, Phys. Rev, B, Submitted (2002).
10. Daewoong Suh, P. Asoka-Kumar, R.H. Dauskardt, Acta Materialia **50**, 537 (2002).
11. K.M. Flores, D. Suh, R. Howell, P. Asoka-Kumar, and R.H. Dauskardt, Materials Transaction, **42**, 619 (2001).
12. K.M. Flores, D. Suh, R.H. Dauskardt , P. Asoka-Kumar, P.A. Sterne, and R.H. Howell, J. of Material Research, in press (2002).
13. P.A. Sterne, P. Asoka-Kumar, J.H. Hartley, R.H. Howell, T.G. Nieh, K.M. Flores, D. Suh, R.H. Dauskardt, Mater. Res. Soc. Sympos. Proc., **644**, L1.3.1 (2001).
14. R.J. Gottschall, Materials Trans., **42**, 548 (2001).
15. A. Inoue, Acta Mater. **48**, 279 (2000).
16. K.P. Gopinathan and C.S. Sunder, in *Metallic Glasses – Production, Properties, and Applications*, p 115 (Trans. Tech., Aedermannsdorf, Switzerland, 1984).
17. S. Matsui, J. Phys. Soc. Japan, **61**, 187 (1992).
18. M. Alatalo, H. Kauppinen, K. Saarinen, M.J. Puska, J. Makinen, P. Hautojärvi, and R.M. Nieminen, Phys. Rev. B **51,** 4176(1995).
19. P. Asoka-Kumar, M. Alatalo, V.J. Ghosh, A.C. Kruseman, B. Nielsen, and K.G. Lynn, Phys. Rev. Lett., **77**, 2097 (1996) 2097.
20. U. Myler, P.J. Simpson, D.W. Lawther, and P.M. Rousseau, J. Vac. Sci. Technol. B **15**, 1(1997).
21. K. Saarinen, T. Laine, S. Kuisma, J. Nissilä, P. Hautojärvi, L. Dobrzynski, J.M. Baranowski, K. Pakula, R. Stepniewski, M. Wojdak, A. Wysmolek, T. Suski, M. Leszczynski, I. Grzegory, and S. Porowski, Phys. Rev. Lett., **79**, 3030 (1997).
22. J. Kuriplach, A.L. Morales, C. Dauwe, D. Sgers, M. Šob, Phys. Rev. B 58, 10475(1998).
23. M.P. Petkov, M.H. Weber, K.G. Lynn, R.S. Crandall, V.J. Ghosh, Phys. Rev. Lett., **82**, 3819(1999).
24. P. Asoka-Kumar, J. Hartley, R. Howell, P.A. Sterne, and T.G. Nieh, Appl. Phys. Lett., **77**, 1973 (2000).
25. R. Howell, R.A. Alvarez, and M. Stanek, Appl. Phys. Lett. **40**, 751 (1982).
26. R. Ley, Hyperfine Interactions, **109**, 167 (1997).
27. W. Stoeffl, P. Asoka-Kumar, R.H. Howell, Appl. Surf. Sci., **149**, 1 (1999).
28. P. Asoka-Kumar, R. Howell, W. Stoeffl, and D. Carter, *Application of Accelerators in Research and Industry*, Eds. J.L. Duggan, I.L. Morgan, (American Institute of Physics, New York 1999).